

IMPULSIVE TENSION OF HEXANE AND GLYCEROL UNDER SHOCK-WAVE LOADING

A. V. Utkin, V. A. Sosikov, and A. A. Bogach

UDC 532.538 + 539.593

The strength of hexane and glycerol was measured under impulsive tension produced by interaction of a triangular compression pulse with a free surface. The tests were performed for strain rates of 10^4 – 10^5 sec $^{-1}$. It is established that the strength of hexane is equal to 14 MPa and does not depend on the strain rate, whereas the strength of glycerol increases from 57 to 142 MPa with an order of magnitude increase in the strain rate. The possibility of using the model of homogeneous nucleation to interpret the data obtained is discussed.

Key words: *shock-wave action, shock waves, fluid failure, cavitation.*

According to [1, 2], fluids can sustain considerable tensile stresses reaching 0.1–1.0 GPa. In this case, the continuity of the material is disturbed by the appearance of pores via the mechanism of homogeneous cavitation. At the same time, static tests recorded smaller stresses [3], which is explained by the presence of heterogeneous sites in real fluids that give rise to pore growth. Among the various impurities contained in fluids, only bubbles, existing independently or in small cracks of undiluted particles, can have a considerable effect on the fluid strength.

Real conditions of fluid failure during homogeneous nucleation can be simulated using dynamic extension. In the present study, dynamic extension of the fluids was performed using spalling phenomena that occur in the reflection of compression pulses from the free surface of the material studied [4]. An advantage of this approach is that the fracture caused by short-duration pulses is volume (the effect of boundaries is eliminated) and occurs in a thin layer of the material. This leads to a decreased number of heterogeneous sites that can influence fluid failure. Moreover, precompression in a shock wave is likely to result in a partial collapse of pores, which also activates homogeneous nucleation.

Impulsive extension of fluids by shock-wave loading was used to study the cavitation of glycerol [5, 6], water [7–9], ethylene glycol [7], ethanol [8], and mercury [10]. For glycerol, which has been studied most extensively, the dependence of the spall strength on temperature was determined for the temperature range $T = 220$ – 350 K [6]. It was shown that the spall strength decreases from 250 MPa at $T = 262$ K to 34 MPa at $T = 350$ K. Carlson and Levine [6] explain the results obtained within the unsteady theory of homogeneous nucleation. The strain rate in the experiments of [6] was varied severalfold and was of the order of $0.1 \mu\text{sec}^{-1}$. At the same time, the dependence of the strength on the strain rate reflects the failure mechanism. Of special interest is a comparison of the special features of fluid failure with various relaxation times because it can give an insight into the effect of relaxation processes on the character of fracture. In the present paper, we describe experimental measurements of the spall strengths of hexane and glycerol over a wide range of compression-pulse times and discuss the possibility of using the model of homogeneous nucleation to interpret the data obtained.

Experimental Results. A diagram of the experiments is shown in Fig. 1. Shock waves were generated by the action of an aluminum impactor (1) 0.2–2.0 mm thick accelerated by explosion products to velocities of 500–600 m/sec [4] upon the Plexiglas dish bottom 2 mm thick. The loading conditions were varied by changing the impactor thickness h_i and the fluid-layer thickness h_l (see Table 1). In experiment Nos. 6 and 8, the compression pulse was formed by the impact of explosion products on a copper plate 20 mm thick. The velocity was recorded

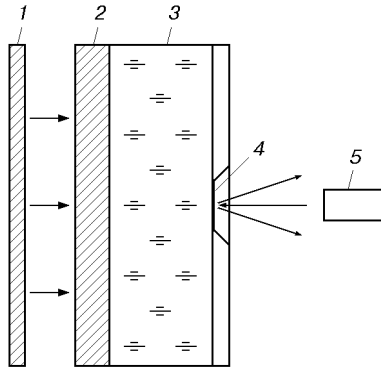


Fig. 1. Diagram of the experiments: 1) impactor; 2) plate; 3) fluid; 4) aluminum foil; 5) VISAR laser interferometer.

TABLE 1

Experiment No.	h_i , mm	h_l , mm	P_0 , MPa	ΔW , m/sec	P_s , MPa	$\dot{\epsilon} \cdot 10^{-4}$, sec $^{-1}$
Hexane						
1	0.2	4	162	39 ± 2	14.0 ± 0.7	12
2	0.2	4	162	—	—	12
3	0.4	4	425	43 ± 2	15.4 ± 0.7	15
4	0.4	4	425	—	—	15
5	0.4	8	227	39 ± 2	14.0 ± 0.7	5
6	—	8	454	34 ± 2	13.2 ± 0.7	2
7	2.0	8	719	43 ± 2	15.4 ± 0.7	3
Glycerol						
8	—	8	1222	48 ± 2	57 ± 2	1.5
9	0.2	1	782	119 ± 2	142 ± 7	20.8
10	0.4	8	652	78 ± 2	93 ± 0.7	6.2

by a VISAR laser interferometer [6] with an interferometer constant of 80.8 m/sec; the measurement error was 2 m/sec and the time resolution was approximately 4 nsec. The laser beam was reflected from an aluminum foil 7 μm thick which separated water from air. The geometrical parameters of the setup (diameter of the impactor flat section more than 40 mm) ensured one-dimensional loading conditions and ruled out the arrival of the lateral unloading wave during the experiment. On reaching the free surface, the compression pulse was triangular, which was determined in separate experiments performed on a setup similar to that shown in Fig. 1 but the foil was submerged in the fluid.

Hexane. In the experiments, we used hexane C_6H_{14} with density $\rho_0 = 0.66 \text{ g/cm}^3$ at an initial temperature of 292 K (speed of sound $c_0 = 1.083 \text{ km/sec}$). The experimental results are given in Figs. 2 and 3 (curve numbers correspond to the experiment numbers in Table 1).

Upon reaching the free surface, the shock wave gives rise to a jump in the surface velocity to W_0 , which is twice the value of the mass velocity in the shock wave. A centered rarefaction wave propagates into hexane and interacts with the incident unloading wave, thus causing internal spalling fracture. During the fracture, the tensile stresses relax to zero, thus producing a compression wave, which arrives at the free surface in the form of a spalling pulse. The indicated features are observed on the velocity profiles in Figs. 2 and 3. Mass velocities in the incident compression pulses were measured in test Nos. 2 and 4, and free-surface velocities were measured in test Nos. 1 and 3. A comparison of profiles 1 and 2 and 3 and 4 shows that the velocity doubling rule is fulfilled with good accuracy. This implies that cavitation is absent at the foil–hexane interface, which would otherwise impair adhesion between the foil and hexane and, consequently, result in a less steepness of the velocity drop immediately after the shock wave has reached the free surface.

The effect of the fracture kinetics on unloading can be determined by measuring the incident-pulse parameters. For example, a break is recorded in the phase of decreased free-surface velocity (curve 3) approximately 0.18 μsec after the shock wave has arrived at the free surface (see Fig. 2). This phenomenon can be due to the initial-pulse shape or cavitation. A comparison of curves 3 and 4 shows that in this case, an inflection also exists on curve 4, and, hence, it cannot be due to the kinetics of pore growth.

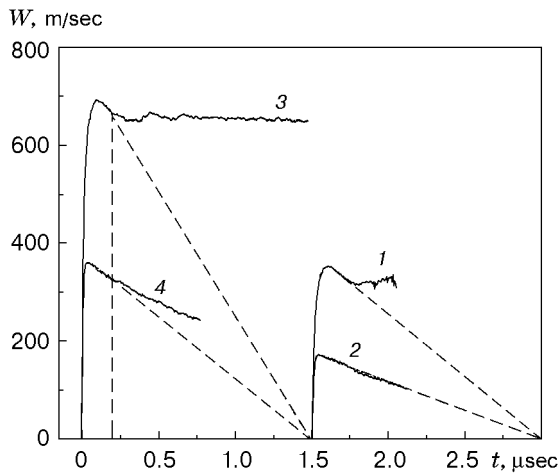


Fig. 2

Fig. 2. Mass velocities (2 and 4) and free-surface velocities (1 and 3) for hexane (dashed curves show the extrapolated free-surface velocity in the absence of cavitation).

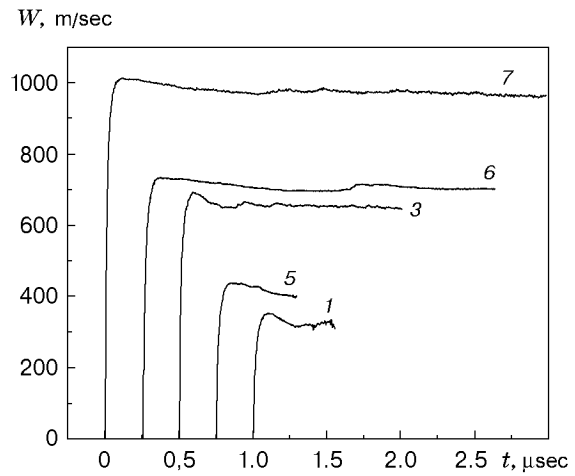


Fig. 3

Fig. 3. Free-surface velocity versus time in experiments with hexane.

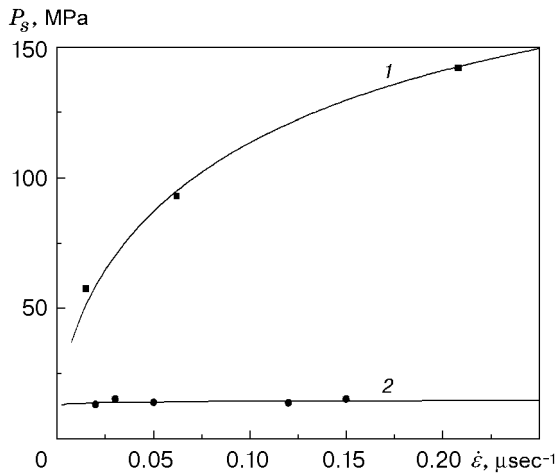


Fig. 4

Fig. 4. Strength versus the strain rate for glycerol (1) and hexane (2): the points refer to experimental data and the curves refer to calculation results.

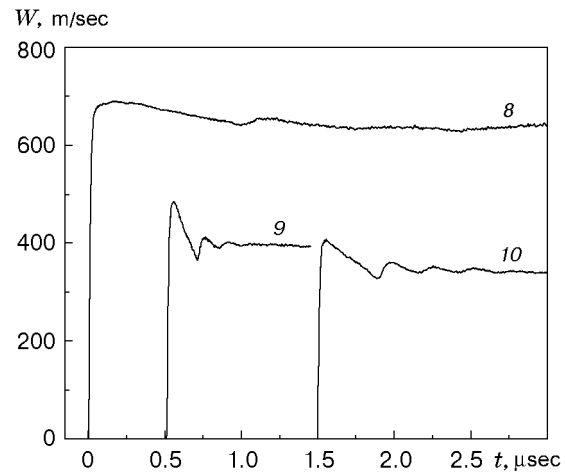


Fig. 5

Fig. 5. Free-surface velocity versus time in experiments with glycerol.

The spall strength P_s , which characterizes the maximum tensile stresses in a specimen, was determined from the minimum velocity W_{\min} attained in front of the spalling pulse [4]: $P_s = 0.5\rho_0 c_0 \Delta W$, where $\Delta W = W_0 - W_{\min}$.

Figure 3 shows experimental curves of the free-surface velocity of hexane versus time for the case where the amplitude of the compression pulse P_0 increases in the range of 162–719 MPa and the strain rate in the unloading part of the pulse is $\dot{\epsilon} = (dW/dt)/(2c_0) = 2 \cdot 10^4 - 15 \cdot 10^5 \text{ sec}^{-1}$. The values of the maximum pressure P_0 shown in Table 1 were calculated from the shock adiabat $D = 1.083 + 2.23u - 0.197u^2$ [11], where the shock-wave velocity D and the mass velocity u are expressed in kilometers per second. The strength values are given in Table 1. Figure 4 shows a curve of $P_s(\dot{\epsilon})$. It is seen that the values of P_s are virtually constant over the entire range of strain rates. The tensile stresses in test No. 5 can slightly exceed 14 MPa since the minimum velocity recorded is due not to a spall pulse but to the second shock wave resulting from collision of a massive steel attenuator following the impactor with hexane.

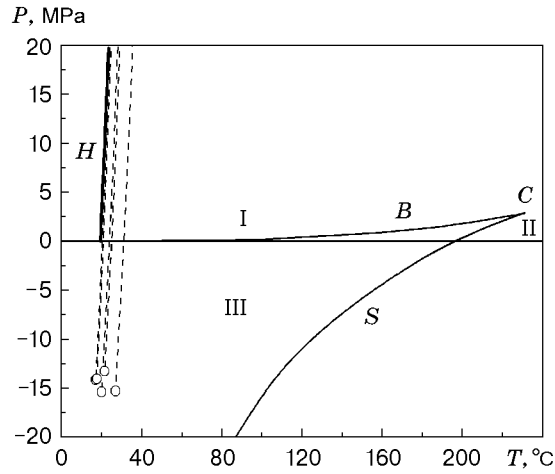


Fig. 6. Phase plane in the coordinates P - T for hexane in the metastability region: H is the shock adiabat, B is the binodal, S is the spinodal, C is the critical point, the dashed curves correspond to isentropes, and the circles are experimental data; regions I and II refer to the fluid and vapor; III is the metastability region.

Glycerol. In the experiment, we used glycerol ($C_3H_8O_3$) with a density of 1.26 g/cm^3 at a temperature of 292 K (speed of sound 1.895 km/sec). The experimental results are shown in Figs. 4 and 5 (curve numbers on the curves in Fig. 5 correspond to the experiment numbers in Table 1). The amplitude of the compression pulse was varied by less than twofold and the strain rate varied from $1.5 \cdot 10^4$ to $2 \cdot 10^5 \text{ sec}^{-1}$. In pressure calculations, a shock adiabat $D = 1.895 + 3.05u - 0.97u^2$ ($u < 1 \text{ km/sec}$) was used to approximate the data of [12]. The free-surface velocity profiles for hexane and glycerol agree qualitatively; however, the spalling pulse and the subsequent velocity oscillations due to the wave circulation between the specimen surface and the fracture region are more clearly pronounced for glycerol. This is obviously explained by the sharper boundaries of the cavitation zones in glycerol. Of interest is a comparison of the velocity profiles for glycerol with those for water [9]. The velocity profiles for water show a steep (with a characteristic time of 30 nsec) spalling-pulse front. The amplitude of this front virtually coincides with the minimum velocity. Since the steepness of the spalling pulse is determined by the rate of pore growth [13], cavitation proceeds more slowly in hexane and glycerol than in water.

The value of the spalling pulse in glycerol exceeds that in hexane by an order of magnitude, and the dependence $P_s(\dot{\epsilon})$ is very strong for hexane, which is typical neither of hexane nor water. We also note that the spall strength of glycerol for strain rates of the order of 10^5 sec^{-1} is approximately 100 MPa , which coincides with the results obtained by Carlson and Levine [6]. This coincidence is not obvious because in [6] compression pulses were generated by impact of electron beams on a condensed target. In this case, the initial pressure profile consisted of a compression pulse and a subsequent extension pulse, in which the amplitude of negative pressures can be equal to the shock-wave amplitude. Therefore, by the moment the unloading wave from the free surface arrives at the spalling plane, the substance in this plane is already subjected to negative pressure. However, the spall strength varies only slightly in this case.

Discussion of Experimental Results. For negative pressures produced by pulsed extension, the fluid enters the region of a metastable state (Fig. 6), whose lifetime depends on the purity of the liquid and extension conditions. Figure 6 shows the phase plane of hexane in a two-phase water-vapor region. The fluid spinodal S and the phase-equilibrium curve (binodal B) plotted using the data of [3] bound the metastability region.

In our experiment, hexane was compressed along the shock adiabat H to the maximum pressure P_0 indicated in Table 1 and then unloaded isentropically to the states shown by circles in Fig. 6. To calculate the shock adiabat and isentropes, we used the dependence of the speed of sound on temperature and pressure [14]. The metastable state fails as a result of growth of pores, which always exist in a fluid and are generated by thermal fluctuation processes. Bogach and Utkin [9] showed that the pores existing in a fluid do not affect the initiation of cavitation and the experimental weak dependence of P_s on the strain rate $\dot{\epsilon}$ for water is explained by homogeneous nucleation.

We now consider the effect of homogeneous nucleation on an increase in porosity under spalling conditions. According to the thermodynamic theory of fluctuations [1], the rate J of formation of pores of the critical radius $R_c = 2\sigma/P_s$ (σ is the surface-tension coefficient) per unit volume is described by the kinetic equation. In the general case, the kinetic equation is unsolvable; hence, the following steady-state solutions are usually considered:

$$J_0 = N_0 \frac{\sigma}{\eta} \sqrt{\frac{\sigma}{kT}} \exp\left(-\frac{16\pi\sigma^3}{3P_s^2 kT}\right), \quad (1)$$

where N_0 is the number of molecules per unit volume of the fluid, η is the viscosity, T is the temperature, and k is the Boltzmann constant. Studies of the effect of the pore growth kinetics on the dynamics of wave interactions under spalling conditions show [15] that a minimum on the free-surface velocity profile is formed when the rate of pore growth, which is proportional to $R_c^3 J_0$ [9], far exceeds the critical value, which depends on the strain rate in the unloading part of the pulse: $R_c^3 J_0 = \gamma \dot{\epsilon}$, where $\gamma \approx 1$.

Assuming that an increase in porosity is caused mostly by nucleation rather than viscosity growth, we can determine the character of the dependence of the spall strength on the strain rate [15]:

$$P_s \approx A/\sqrt{\ln(B/\dot{\epsilon})}. \quad (2)$$

Here A and B are constants that depend on temperature both explicitly and via the viscosity and surface-tension coefficient. The lower bound of B is estimated to be of the order of 10^{13} sec^{-1} . Curve 2 in Fig. 4 is plotted by relation (2) for $A = 85 \text{ MPa}$ and $B = 10^{13} \text{ sec}^{-1}$ and describes adequately experimental data for hexane. This curve shows that the development of cavitation in glycerol, where P_s depends strongly on $\dot{\epsilon}$, cannot be explained only within the theory of homogeneous nucleation. Indeed, this result means that, first, the steady-state solution is inapplicable in this case to interpret experimental data and, second, the effect of the strain rate on the viscosity of glycerol must be taken into account. We consider unsteady evolution of the flow of nuclei in the approximation proposed by Zel'dovich [1]:

$$J = J_0 \exp(-\tau/t). \quad (3)$$

Here τ is the relaxation time required to establish a steady distribution of the nuclei. According to the estimates of [3], the relaxation time for hexane is of the order of 1 nsec, which is well below the characteristic extension time in the experiments conducted. In this case, the steady-state solution for the frequency of homogeneous nucleation (1) is applicable.

The relaxation time of glycerol is an exponential function of temperature and is of the order of $1 \mu\text{sec}$ at $T = 292 \text{ K}$ [6], which is comparable with the characteristic extension time in the experiments. Therefore, relation (3) should be used to determine the dependence $P_s(\dot{\epsilon})$. Then, assuming that $R_c^3 J \sim \dot{\epsilon}$ and $t \sim 1/\dot{\epsilon}$, we have

$$P_s = A/\sqrt{\ln(B \exp(-\alpha\dot{\epsilon})/\dot{\epsilon})}, \quad (4)$$

where the constants A and B have the same meaning as in formula (2); $\alpha \sim \tau$. In addition, the strong dependence of the glycerol viscosity on temperature in the vicinity of the freezing point ($T = 291 \text{ K}$) [6] suggests the validity of the temperature–time superposition principle, according to which the change in the viscous properties of materials upon a decrease in the time of action is the same as that upon a decrease in temperature. Therefore, to estimate the effect of the strain rate on the viscosity for times comparable to τ , we use the simplest relaxation law: $\dot{\eta} \sim -\eta/\tau$. Then, $\eta \sim \exp(-t/\tau) \sim \exp(-1/(\dot{\epsilon}\tau))$, i. e. an increase in the strain rate, as well as a temperature drop, leads to a significant increase in the viscosity. Since the constant $B \sim 1/\eta \sim \exp(1/(\dot{\epsilon}\tau))$, relation (4) can be written as

$$P_s = A/\sqrt{\ln(B \exp(-\alpha\dot{\epsilon} + \beta/\dot{\epsilon})/\dot{\epsilon})}, \quad (5)$$

where $\beta \sim 1/\tau$ is a constant.

An analysis of relation (5) shows that in the range of $\dot{\epsilon}$ of interest, the constant α has almost no effect on P_s , and, hence, unsteadiness in the evolution of the flow of nuclei does not determine the character of the dependence $P_s(\dot{\epsilon})$. At the same time, the effect of the constant β is significant. Figure 4 shows curve (5) for $A = 970 \text{ MPa}$, $B = 10^{15} \text{ sec}^{-1}$, $\beta = 5 \mu\text{sec}$, and $\alpha = 0$, which adequately describes the experimental data for glycerol.

Thus, the model of homogeneous nucleation describes the experimental difference between the dependences of the strength of hexane and glycerol on the strain rates. In this case, in the examined range of $\dot{\epsilon}$ for both fluids, one can use the steady-state solution for the rate of pore formation. However, for glycerol, the dependence of the viscosity on the strain rate must be taken into account. This is due to the fact that the initial temperature of glycerol coincides with the freezing point; in the vicinity of this point, the relaxation properties of the medium are clearly manifested and the relaxation time is comparable to the characteristic extension time in the experiments conducted.

REFERENCES

1. Ya. B. Zel'dovich, "Theory of formation of a new phase. Cavitation," *Zh. Éksp. Teor. Fiz.*, **12**, Nos. 11/12, 525–538 (1942).
2. M. Kornfel'd, *Elasticity and Strength of FLuids* [in Russian], Gostekhteorizdat, Moscow–Leningrad (1951).
3. V. P. Skripov, *Metastable Liquids* [in Russian], Nauka, Moscow (1972).
4. G. I. Kanel', S. V. Razorenov, A. V. Utkin, and V. E. Fortov, *Shock-Wave Phenomena in Condensed Media* [in Russian], Yanus-K, Moscow (1996).
5. D. C. Erlich, D. C. Wooten, and R. C. Crewdson, "Dynamic tensile failure of glycerol," *J. Appl. Phys.*, **42**, No. 13, 5495–5502 (1971).
6. G. A. Carlson and H. S. Levine, "Dynamic tensile strength of glycerol," *J. Appl. Phys.*, **46**, No. 4, 1594–1601 (1975).
7. P. L. Marston and B. T. Urgan, "Rapid cavitation induced by the reflection of shock waves," in: *Proc. of the Conf. of the Amer. Phys. Soc. on Shock Waves in Condensed Matter* (Spokane, Washington, July 22–25, 1985), Plenum Press, New York (1986), pp. 401–405.
8. A. N. Dremin, G. I. Kanel', and S. A. Koldunov, "Spallation in water, ethanol, and acrylic plastic," in: *Proc. III All-Union Symp. on Combustion and Explosion* (Leningrad, July 5–10, 1971), Nauka, Moscow (1972), pp. 569–574.
9. A. A. Bogach and A. V. Utkin, "Strength of water under pulsed loading," *J. Appl. Mech. Tech. Phys.*, **41**, No. 4, 752–758 (2000).
10. G. A. Carlson, "Dynamic tensile strength of mercury," *J. Appl. Phys.*, **46**, No. 9, 4069–4070 (1975).
11. J. M. Walsh and M. H. Rice, "Dynamic of liquids from measurements on strong shock waves," *J. Chem. Phys.*, **26**, No. 4, 321–337 (1957).
12. R. D. Dick, "Shock compression data for liquids. 3. Substituted methane compounds, ethylene glycol, glycerol, and ammonia," *J. Chem. Phys.*, **74**, No. 7, 4053–4061 (1981).
13. A. V. Utkin, "Effect of initial failure rate on the formation of a spalling pulse," *J. Appl. Mech. Tech. Phys.*, **34**, No. 4, 578–584 (1993).
14. T. S. Khasanshin and A. P. Shchemelev, "Speed of sound in liquid *n*-alkanes, *Teplofiz. Vys. Temp.*, **39**, No. 1, 64–71 (2001).
15. A. V. Utkin, "Determination of the constants of spall-fracture kinetics of materials using experimental data," *J. Appl. Mech. Tech. Phys.*, **38**, No. 6, 952–960 (1997).